Model Compound Studies Related to Peroxidases. Mechanisms of Reactions of Hemins with Peracids

T. G. Traylor,* William A. Lee, and Dennis V. Stynes

Contribution from the Department of Chemistry, D-006, University of California, San Diego, La Jolla, California 92093. *Received September 16, 1982*

Abstract: A peroxidase model system employing various model hemin compounds as catalysts, *m*-chloroperbenzoic acid as the principal oxidant, and tri-*tert*-butylphenol as the substrate is described. The kinetic effects of a proximal imidazole and distal carboxylate on the rates of intermediate formation are examined by using propionic acids and imidazole side chains attached to the hemin. Collidine and collidine buffers are used to study pH effects and general base catalysis on the rate of intermediate formation. Proximal base acceleration and intramolecular general base catalysis are demonstrated. In addition, the dependencies on solvent composition and oxidant structure are discussed.

The peroxidases are a class of iron(III) porphyrin containing proteins that catalyze the oxidation of substrates by hydrogen peroxide.[1] Horseradish peroxidase (HRP), the most thoroughly studied and perhaps representative enzyme of this class, reacts with hydrogen peroxide, hydroperoxides[2] or peracids[3] to form two distinct intermediates known as compounds I[4] and II.[5] The reactivities of these intermediates are independent of the nature of the oxidant.[6]

The HRP intermediates have been isolated and studied, both spectroscopically and kinetically. Compound I is a green (λ_{max} 410, 655 nm)[7] species containing two oxidizing equivalents above the Fe(III) state. Recent evidence (ESR,[8] ENDOR,[9] UV-visible,[10] and NMR[11]) suggests that it is an Fe(IV) porphyrin cation radical

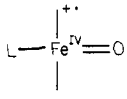

rather than the Fe(V) species

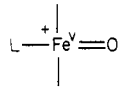

Compound II is red (λ_{max} 420, 527, 554 nm),[12] contains one oxidizing equivalent, and is usually written as

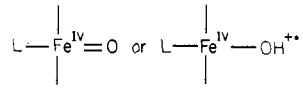

Both intermediates rapidly oxidize phenols and aromatic amines ($k \sim 10^7$ M^{-1} s^{-1}).[13] The accepted enzymatic cycle was originally proposed by George.[14]

$$\text{HRP} + \text{H}_2\text{O}_2 \rightarrow \text{HRP-I} \quad (1)$$

$$\text{HRP-I} + \text{AH}_2 \rightarrow \text{HRP-II} + \text{AH}\cdot \quad (2)$$

$$\text{HRP-II} + \text{AH}_2 \rightarrow \text{HRP} + \text{AH}\cdot \quad (3)$$

Like hemoglobin and myoglobin, the peroxidases contain an iron protoporphyrin IX with a proximal-bound histidine in their active site.[15] In contrast to the dioxygen-carrying proteins, the peroxidases are Fe(III) hemoproteins in their resting state, are reduced with difficulty to the Fe(II) state,[16] and are much more reactive toward hydrogen peroxide than is myoglobin.[1,3,17] Furthermore, the rates of reaction of peracids and alkylhydroperoxides or hydrogen peroxide with HRP are rather similar[18-20] whereas peracid derivatives are usually much more easily cleaved at the oxygen–oxygen bond than are hydroperoxide derivatives.[21,22] These observations lead to the conclusion that some special catalysis of O–O bond breaking is occurring in the HRP reaction.

Three questions concerning the sequence of reactions above can be addressed with synthetic model compounds: (1) How is the high valent intermediate formed? (2) What is its structure? (3) What are the mechanisms of its reaction with substrates? We will address the first question here and the third in a separate publication. The second question has been answered, at least in part, in other laboratories. Recent studies of Groves and co-workers[23] and La Mar and Balch and their co-workers[24] indicate that the first intermediate, analogous to HRP compound I, formed upon reaction of a hemin with iodosylbenzene or peracids at low temperature is an Fe(IV) porphyrin cation radical[25] and that the one-electron reduced form of this intermediate is observable at low temperature. Both of these intermediates react with selected substrates but the mechanisms of these reactions have not been studied in detail.

Portsmouth and Beal[26] and Jones and co-workers[27-29] have studied the kinetics of reaction of peracids with protohemin and other simple hemins in aqueous solution, showing that the rate

(1) Dunford, H. B.; Stillman, J. S. *Coord. Chem. Rev.* **1976**, *19*, 187-251.
(2) Chance, B. *Arch. Biochem. Biophys.* **1952**, *37*, 235-239.
(3) (a) Schonbaum, G. R.; Lo, S. *J. Biol. Chem.* **1972**, *247*, 3353-3360. (b) Morrison, M.; Schonbaum, G. R. *Annu. Rev. Biochem.* **1976**, *45*, 861-888.
(4) Theorell, H. *Enzymologia* **1941**, *10*, 250-252.
(5) Keilin, D.; Mann, T. *Proc. R. Soc. London, Ser. B* **1937**, *122*, 119-133.
(6) George, P. *Biochem. J.* **1953**, *55*, 220-230.
(7) Chance, B. *Arch. Biochem. Biophys.* **1949**, *21*, 416-430.
(8) Aasa, R.; Vänngard, T.; Dunford, H. B. *Biochim. Biophys. Acta* **1975**, *391*, 259-264.
(9) Roberts, J. E.; Hoffman, B. M.; Rutter, R.; Hager, L. P. *J. Biol. Chem.* **1981**, *256*, 2118-2121.
(10) Dolphin, D.; Forman, A.; Borg, D. C.; Fajer, J.; Felton, R. H. *Proc. Natl. Acad. Sci. U.S.A.* **1971**, *68*, 614-618.
(11) LaMar, G. N.; deRopp, J. S. *J. Am. Chem. Soc.* **1980**, *102*, 395-397.
(12) Chance, B. *Science (Washington, D.C.)* **1949**, *109*, 204-208.
(13) Job, D.; Dunford, H. B. *Eur. J. Biochem.* **1976**, *66*, 607-614.
(14) George, P. *Adv. Catal.* **1952**, *4*, 367-428.
(15) Brill, A.; Sandberg, H. *Biochemistry* **1968**, *7*, 4254-4260.
(16) Yamada, H.; Makino, R.; Yamazaki, I. *Arch. Biochem. Biophys.* **1975**, *169*, 344-353.
(17) Bennett, L. *Prog. Inorg. Chem.* **1973**, *18*, 1-176.
(18) Wittenberg, J.; Noble, R.; Wittenberg, B.; Antonini, E.; Brunori, M.; Wyman, J. *J. Biol. Chem.* **1967**, *242*, 626-634.
(19) King, N. K.; Winfield, M. E. *J. Biol. Chem.* **1963**, *238*, 1520-1528.
(20) Paul, K. G.; Ohlsson, P. I.; Wold, S. *Acta Chem. Scand., Ser. B* **1979**, *B33*, 747-754.
(21) Bartlett, P. D.; Traylor, T. G. *J. Am. Chem. Soc.* **1961**, *83*, 856-861.
(22) Hedaya, E.; Winstein, S. *J. Am. Chem. Soc.* **1967**, *89*, 1661-1672.
(23) (a) Groves, J. T.; Haushalter, R. C.; Nakamura, M.; Nemo, T. E.; Evans, B. J. *J. Am. Chem. Soc.* **1981**, *103*, 2884-2886. (b) Groves, J. T.; Nemo, T. E.; Meyers, R. S. *Ibid.* **1979**, *101*, 1032-1033.
(24) Chin, D.; Del Gaudio, J.; La Mar, G. N.; Balch, A. L. *J. Am. Chem. Soc.* **1977**, *99*, 5486-5488.
(25) Felton, R. H.; Owen, G. S.; Dolphin, D.; Fajer, J. *J. Am. Chem. Soc.* **1971**, *93*, 6332-6334.
(26) Portsmouth, D.; Beal, E. A. *Eur. J. Biochem.* **1971**, *19*, 479-487.
(27) Jones, P.; Mantle, D.; Davies, D.; Kelley, H. C. *Biochemistry* **1977**, *16*, 3974-3978.
(28) Kelly, H.; Davies, D.; King, M.; Jones, P. *Biochemistry* **1977**, *16*, 3543-3549.
(29) Jones, P.; Mantle, D.; Wilson, I. *J. Chem. Soc., Dalton Trans.* **1983**, 161-164.

0002-7863/84/1506-0755$01.50/0 © 1984 American Chemical Society

Table I. Effect of Hemin Structure on the k_2 for Intermediate Formation at 25 °C in CH_3OH[a]

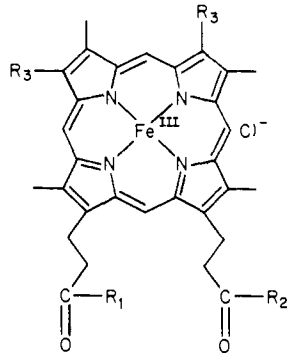

hemin	R_1[b]	R_2[b]	R_3	k_2, M^{-1} s^{-1} [c]
1$^+Cl^-$, protohemin mono-3-(1-imidazoyl)propylamide monomethyl ester	-NHCH$_2$CH$_2$CH$_2$-(N)	-OCH$_3$	vinyl	(7.6 ± 0.2) × 10^3
mesohemin-1$^+Cl^-$, mesohemin mono-3-(1-imidazoyl)propylamide monomethyl ester	-NHCH$_2$CH$_2$CH$_2$-(N)	-OCH$_3$	ethyl	(7.4 ± 0.8) × 10^3
2$^+Cl^-$, mesohemin 2-(4-imidazoyl)-ethylamide monodioctylamide	-NHCH$_2$CH$_2$-(NH)	-N[-CH$_2$(CH$_2$)$_6$-CH$_3$]$_2$	ethyl	(1.7 ± 0.3) × 10^4
3$^+Cl^-$, mesohemin mono-3-[1-(2-methylimidazoyl)propyl]amide monomethyl ester	-NHCH$_2$CH$_2$CH$_2$-(N, CH$_3$)	-OCH$_3$	ethyl	(1.4 ± 0.3) × 10^4
4$^+Cl^-$, protohemin dimethyl ester	-OCH$_3$	-OCH$_3$	vinyl	(2.0 ± 0.4) × 10^3
5$^+Cl^-$, protohemin bis(dimethylamide)	-N(CH$_3$)$_2$	-N(CH$_3$)$_2$	vinyl	2.0 × 10^3
6$^+Cl^-$, protohemin bis[3-(1-imidazoyl)propylamide]	-NHCH$_2$CH$_2$CH$_2$-(N)	-NHCH$_2$CH$_2$CH$_2$-(N)	vinyl	(4.6 ± 0.5) × 10^3
7$^+Cl^-$, protohemin mono-3-(1-imidazolyl)propylamide	-NHCH$_2$CH$_2$CH$_2$-(N)	-OH	vinyl	1.4 × 10^5 [d]
8$^+Cl^-$, protohemin monomethyl ester	-OCH$_3$	-OH	vinyl	5 × 10^4 [d]
9$^+Cl^-$, protohemin	-OH	-OH	vinyl	1.0 × 10^5
Fe(III) tetraphenylporphyrin				1.9 × 10^3
Fe(III) tetramesitylporphyrin				(1.9 ± 0.1) × 10^3

[a] [Tri-*tert*-butylphenol] ≈ 10^{-2} M; $[MCPBA]_{initial} \approx 10^4$ M. [b] All compounds in which R_1 and R_2 differ are equimolar mixtures of compounds with R_1 and R_2 interchanged, resulting from direct synthesis from protohemin chloride or mesohemin chloride. [c] Observed first-order rate constant for hemin concentration. [d] A similar rate constant was observed in the presence of 0.005 M collidine at pH 8.25.

of reaction depends upon hemin concentration and peracid. However, the reaction is complicated by the dimerization of hemin in aqueous solution and by the fact that the observed intermediate seemed to be an oxidized hemin dimer[27] rather than the monomeric species reported by Groves et al.[23]

In order to clarify the mechanisms of the reaction of peracids, hydroperoxides, and hydrogen peroxide with peroxidases, we have developed model systems that resemble the active site of HRP and studied their catalytic behavior in organic or aqueous organic solvents where aggregation is absent. We have used a rapid one-step production of a stable phenoxy radical[30] both to trap the high valent intermediate as it is formed and to assay the disappearance of the peroxy function. The simplifications introduced in this system have allowed us to establish the mode of O–O bond breaking as well as some of the factors involved in the HRP catalysis of this process.

Results

Hemin Catalysts. The iron(III) porphyrin catalysts used in this study are shown in Table I. All have been characterized elsewhere. Mesohemin compounds analogous to 2$^+Cl^-$ were previously prepared and characterized by Castro.[31] The spectroscopic behavior of his compounds in methanol agrees well with those observed here. In the protohemin and mesohemin series (**1**, **2**, **3**, **7**, **9**) the UV–visible spectra of the Fe(II) forms are definitive for the presence of one and only one chelating side arm.[32] The ligation states of the Fe(III) forms of these compounds are solvent dependent and sensitive to changes in basicity or acidity of the solvent, resulting in equilibria among the hydroxy form, μ-oxo form, the chelated form, and the base-protonated hemin form.

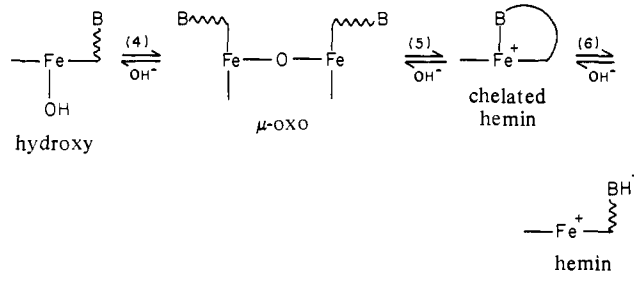

In methanol the spectrum of 1$^+Cl^-$ resembles that of protohemin dimethyl ester (4$^+Cl^-$), suggesting either that methanol has shifted the equilibrium toward the base-dissociation species with methanol coordinated or that the monoimidazole and dimethanol species have the same spectrum. However, the availability of the chelating imidazole for binding is clearly demonstrated by the titration of

(30) Forrester, A. R.; Hay, J. M.; Thomson, R. H. "Organic Chemistry of Stable Free Radicals"; Academic: New York, 1968; pp 1–80.
(31) Castro, C. F. *Bioinorg. Chem.* **1974**, *4*, 45–65.
(32) Traylor, T. G.; Chang, C. K.; Geibel, J.; Berzinis, A.; Mincey, T.; Cannon, J. *J. Am. Chem. Soc.* **1979**, *101*, 6716–6731.
(33) Schonbaum, G. R.; Chance, B. *Enzymes* (*3rd Ed.*) **1981**, *13* (C), 363–408.
(34) Yonetani, T., ref 33, pp 345–362.

1^+Cl^- with 1-methylimidazole in methanol. Unlike the diester,

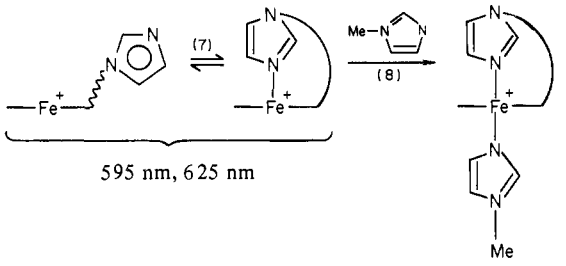

4^+Cl^-, which shows no clean isosbestic behavior in this titration, due to two-step ligation, 1^+Cl^- shows clean isosbestic points at 479, 512, 595, and 665 nm and a k^B for 1-methylimidazole binding of $(4.4 \pm 0.2) \times 10^3$ M^{-1}. This is consistent with a simultaneous binding of internal and external imidazole. The diimidazole hemin (6^+Cl^-) shows a similar bis(imidazole) spectrum, corroborating the internal binding in the hexacoordinated state.

Catalytic Reaction. In order to avoid hemin destruction that is usually consequent upon reaction of natural hemin derivatives with peracid, we have devised a system in which the first-formed intermediate is trapped by a rapidly reacting substrate before it can attack other hemin molecules. A degassed solution of 10^{-3} M *m*-chloroperbenzoic acid (MCPBA) and 0.1 M 2,4,6-tri-*tert*-butylphenol (TBPH) in methanol was found to be stable, showing negligible reaction. Addition of 10^{-6} M chelated protohemin (1^+Cl^-) to the solution caused rapid production of the stable blue tri-*tert*-butylphenoxyl radical, which continued until the peracid was consumed and 2×10^{-3} M radical was formed, as judged by its spectrum. Addition of more peracid produced more radical. Figure 1 shows the spectral changes that occurred when 3×10^{-4} M MCPBA was added to a solution of 10^{-2} M TBPH and 6.3×10^{-6} M 1^+Cl^- in methanol. The spectral difference between the hemin solution and the final solution is that of 6×10^{-4} M phenoxyl radical, demonstrating complete protection against hemin destruction during the production of 100 radicals per hemin molecule. Ratios greater than 10^4 to 1 are easily obtainable without loss of catalyst.

The stoichiometry of the reaction is 2.0 radicals per peracid consumed in methanol and 1.9 radicals per peracid molecule in methylene chloride, both judged by the change in absorption at the phenoxyl radical maxima[30] and the amount of peracid added.

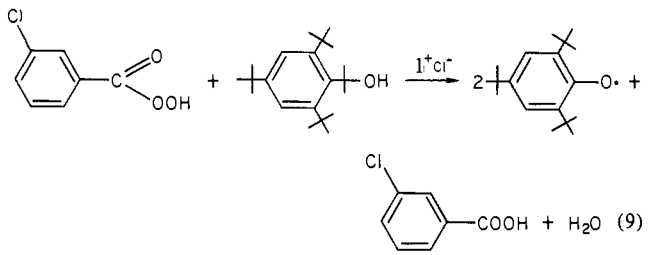

Absence of Homolytic Cleavage of Peracids. The reaction stoichiometry above might be achieved by homolytic cleavage of the peracid followed by radical abstractions. Alkyl carboxyl radicals are known to decarboxylate, even in the presence of phenols.[35] The catalytic reaction described above was repeated by using perlauric acid or perphenylacetic acid instead of MCPBA with similar results. In these latter reactions a stream of nitrogen was swept through the solution and into a barium hydroxide solution during the reaction. Titration of the barium hydroxide revealed less than 1.5% CO_2 formation with perlauric or perphenylacetic acid, indicating less than 1.5% homolytic cleavage during the reaction.

This shows that the reactions studied here proceed by direct heterolytic cleavage to give an acid (or its anion) plus a two-electron oxidized hemin, equivalent to compound I of HRP.

(35) Braum, W.; Rajenbach, L.; Eirich, F. R. *J. Phys. Chem.* **1962**, *66*, 1591–1595.

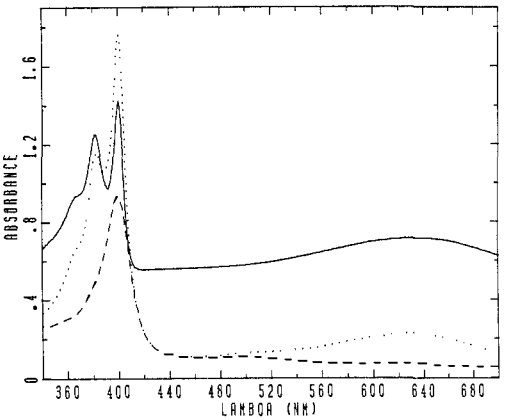

Figure 1. Oxidation of TBPH by MCPBA catalyzed by 1^+Cl^- in methanol. (---) 1^+Cl^- (6.3×10^{-6} M) and TBPH (10^{-2} M); (···) after addition of MCPBA (3×10^{-4} M); (—) the difference spectrum (offset +0.6).

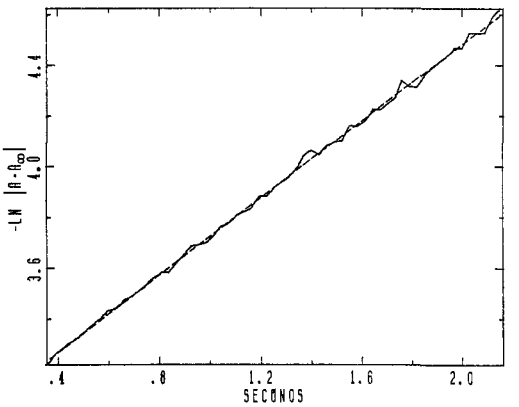

Figure 2. Plot of $-\ln |A_t - A_\infty|$ at 630 nm vs. time for the production of tri-*tert*-butylphenoxyl radical in CH_3OH–H_2O (8:2) at 25 °C. [TBPH] = 2.4×10^{-3} M; [MCPBA] = 1×10^{-4} M; [1^+Cl^-] = 1.5×10^{-6} M. The total ΔOD at 630 nm was 0.04. The solid line represents the data and the dashed line the least-squares fit.

Table II. Rate Constants for TBPH Oxidation in CH_3OH–H_2O (80:20) as a Function of 1^+Cl^-, MCPBA, and TBPH, Measured by Phenoxyl Radical Production, at 25 °C[a]

λ, nm	[1^+Cl^-], M	[MCPBA], M	[TBPH], M	k_{obsd}, s^{-1}	k_2, M^{-1} s^{-1} [b]
398	8.8×10^{-7}	1×10^{-4}	5.0×10^{-4}	0.25	2.8×10^5
630	8.8×10^{-7}	1×10^{-4}	5.0×10^{-4}	0.26	3.0×10^5
398	1.8×10^{-6}	1×10^{-4}	2.5×10^{-3}	0.71	3.9×10^5
630	1.8×10^{-6}	1×10^{-4}	2.5×10^{-3}	0.75	4.2×10^5
630	1.8×10^{-6}	5×10^{-4}	2.5×10^{-3}	0.78	4.3×10^5
630	1.8×10^{-6}	5×10^{-4}	2.5×10^{-3}	0.72	4.0×10^5
398	4.4×10^{-6}	1×10^{-4}	5.0×10^{-4}	1.3	3.0×10^5
630	4.4×10^{-6}	1×10^{-4}	5.0×10^{-4}	1.4	3.2×10^5
398	6.8×10^{-6}	1×10^{-4}	1.0×10^{-3}	2.1	3.1×10^5
630	6.8×10^{-6}	1×10^{-4}	1.0×10^{-3}	2.1	3.1×10^5
398	8.8×10^{-6}	1×10^{-4}	5×10^{-4}	2.2	2.5×10^5
630	8.8×10^{-6}	1×10^{-4}	5×10^{-4}	3.1	3.5×10^5
630	4.4×10^{-6}	5×10^{-5}	5×10^{-4}	1.3	3.0×10^5
398	4.4×10^{-6}	5×10^{-5}	5×10^{-4}	1.2	2.7×10^5
398	4.4×10^{-6}	5×10^{-5}	9.5×10^{-4}	1.3	3.0×10^5

[a] Each k_{obsd} represents the average of at least four separate kinetic runs. [b] $k_b = k_{obsd}/[1^+Cl^-]$.

Kinetics of the Catalytic Reaction. The stoichiometry and high turnover rate established above allows the phenoxyl radical concentration, monitored at 630 or 400 nm, to be used to determine the rate of peracid consumption. A plot of $\ln (A_t - A_\infty)$ vs. time, shown in Figure 2, reveals accurate first-order disappearance of peracid. This first-order behavior was observed under all conditions studied. Table II lists first-order rate constants observed

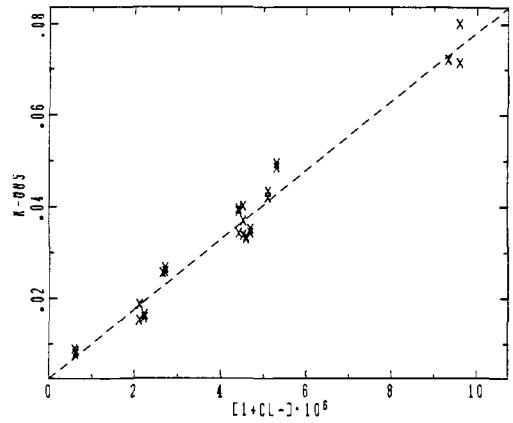

Figure 3. Observed first-order rate constant for intermediate formation as a function of [1^+Cl^-] in CH_3OH at 25 °C. [MCPBA] ≈ 1×10^{-4} M; [TBPH] ≈ 10^{-2} M.

with 1^+Cl^- at various concentrations of reagents. Figure 3 shows a plot of such first-order peracid disappearance constants as a function of hemin concentration [1^+Cl^-] in methanol, demonstrating first-order dependence upon hemin concentration. A similar dependence upon [1^+Cl^-] can be derived from the data in Table II, obtained in aqueous methanol. Similar linear dependence upon hemin concentration was observed with other catalysts. Dividing the first-order rate constants (k_1) in Table II by hemin concentration gives the second-order rate constants (k_2) for this series. These second-order rate constants are, within experimental error, independent of the phenol concentration. The rate law is therefore

$$-\frac{d[RCO_3H]}{dt} = k_2[\text{hemin}][RCO_3H] \qquad (10)$$

which is the same as that proposed by Jones et al.[29] It is rate limited by the formation of the oxidizing intermediate that results from heterolytic oxygen–oxygen bond cleavage, documented above.

Effect of Hemin Structure. The second-order rate constants for catalyzed reactions of *m*-chloroperbenzoic acid with tri-*tert*-butylphenol in methanol at 25 °C are listed in Table I for the hemin compounds studied here. There appears to be no difference in rates of reactions catalyzed by protohemin dimethyl ester (4^+Cl^-), its diamide (5^+Cl^-), tetraphenylhemin chloride, or tetramesitylhemin chloride. Furthermore, chelated protohemin (1^+Cl^-) and chelated mesohemin (mesohemin 1^+Cl^-) react at the same rate.

Attached Base Effects. By comparison with the simple hemin compounds discussed above, all hemin derivatives having covalently attached bases react with accelerated rates. This acceleration occurs even for protohemin and protohemin monomethyl ester in which internal binding of the carboxylate is not possible. The accelerating effects of the attached bases in chelated protohemin (1^+Cl^-) in methylene chloride or benzene are much greater than they are in methanol. These data are summarized in Table III along with the effects of solvent variation. The nature of these effects will be discussed below.

Dependence of Catalytic Rate on Peracid Structure. Table IV lists the rates of TBPH oxidation catalyzed by various peracids and peroxides. These rates are seen to increase as the R in RCO_3H or ROOH becomes more electron withdrawing and therefore to correlate with the acidity of the product acid. This corroborates the heterolytic cleavage in which leaving group stability, related to product acid strength, is expected to be important.[21,22,36]

Solvent Effects. The bimolecular rate constants for chelated protohemin catalyzed oxidation of TBPH were determined in the several solvents shown in Table III. Methanol as solvent slows the reaction as compared to both water–methanol and benzene. This is not a usual solvent effect and it probably reflects the rather strong binding of methanol to Fe(III) porphyrin, indicated from

Table III. Effect of Solvent on the Rate Constants (k_2) for the Formation of the Intermediate in the Reaction of 1^+Cl^- and 4^+Cl^- with MCPBA at 25 °C, Measured by Phenoxyl Radical Production[a]

hemin	solvent	k_2, M^{-1} s^{-1}
1^+Cl^-	CH_3OH	$(7.6 \pm 0.2) \times 10^3$
1^+Cl^-	CH_3OH–H_2O (80:20)	$(3.3 \pm 0.6) \times 10^5$
1^+Cl^-	CH_3OH–H_2O (60:40)[b]	$(9.4 \pm 0.3) \times 10^5$
1^+Cl^-	C_6H_6	$(3.1 \pm 0.3) \times 10^4$
1^+Cl^-	CH_2Cl_2	$(9.7 \pm 1.0) \times 10^4$
1^+Cl^-	DMF	$(1.2 \pm 0.1) \times 10^4$
4^+Cl^-	CH_3OH	$(2.0 \pm 0.4) \times 10^3$ [c]
4^+Cl^-	C_6H_6	$(1.6 \pm 0.2) \times 10^3$ [c]
4^+Cl^-	CH_2Cl_2	$(2.2 \pm 0.2) \times 10^3$ [c]

[a] [Tri-*tert*-butylphenol] ≈ 10^{-2} M; [hemin] ≈ 3×10^{-6} M; [MCPBA] ≈ 10^{-4} M. [b] The phenol oxidized in this experiment was TBP–NH_3^+Cl (see the text). [c] These are observed second-order rate constants k_{obsd}/hemin concentration. If the hemin (4^+Cl^-) is free to react on both sides, then its rate constants should be divided by two, thus doubling the ratio $k_2(1^+Cl^-)/k_2(4^+Cl^-)$.

Table IV. Rate Constants (k_b) for Formation of the Intermediate in the Reaction of 1^+Cl^- with Different Oxidizing Agents at 25 °C[a]

oxidant	k_2, M^{-1} s^{-1}
m-chloroperbenzoic acid	$(7.6 \pm 0.2) \times 10^3$
p-nitroperbenzoic acid	$(9.9 \pm 0.1) \times 10^3$
perlauric acid	$(1.4 \pm 0.1) \times 10^3$
tert-butyl hydroperoxide	4
H_2O_2	12 ± 3

[a] Solvent = CH_3OH; [tri-*tert*-butylphenol] ≈ 10^{-2} M; [1^+Cl^-] ≈ 3×10^{-6} M.

spectroscopic studies discussed above. In order to study the oxidation in 60:40 methanol–water, it was necessary to synthesize the more water-soluble phenol

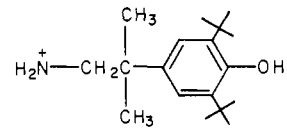

This phenol forms a stable phenoxyl radical with a spectrum like that of TBPH.

General Base Catalysis. In order to study general base catalysis it was necessary to use a base that does not bind to iron. This requirement was demonstrated by using 0.007 M 1-methylimidazole as the base, in which case the reaction was too slow to measure, presumably due to the strong binding of 1-methylimidazole to the hemin,[31] discussed above. We therefore used 2,4,6-trimethylpyridine (collidine), which showed no spectroscopic evidence for binding up to 1 M concentrations in methanol. Collidine buffers were prepared by mixing purified collidine with its hydrochloride and calculating the pH value from the ratio of these compounds and the pK_a of collidine in methanol (7.47), which is the same as its pK_a in water.[37]

Second-order rate constants for the reaction of MCPBA with TBPH catalyzed by chelated protohemin (1^+Cl^-) and chelated histamine (2^+Cl^-) in methanol are plotted against the concentration of free collidine at two buffer ratios in Figures 4 and 5. These plots show the reaction to be dependent upon buffer concentration and independent of pH over the range employed.

Similar results were obtained with protohemin dimethyl ester (4^+Cl^-). Plots of rate constants for three catalysts reacting with MCPBA against collidine concentration are shown in Figure 6. Slopes (k_B) and intercept (k_{int}) values are listed in Table III. The data for 7^+Cl^-, 8^+Cl^-, and 9^+Cl^- are much less accurate than those for compounds without free carboxylate groups. Thus, although a slope for 8^+Cl^-, which is equal to that for 4^+Cl^-, would not be detected within our experimental error, a slope equal to or greater than that for 2^+Cl^- would be detected. Therefore, the monoacid

(36) Bruice, T. C. *J. Chem. Soc., Chem. Commun.* **1983**, 14–15.

(37) Rochester, C. H. *J. Chem. Soc. B* **1967**, 33–36.

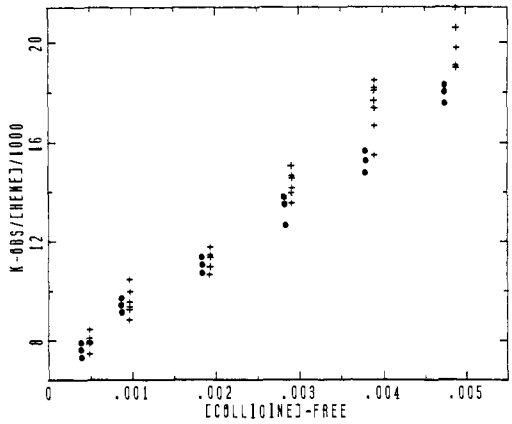

Figure 4. Rate of intermediate formation between $\mathbf{1}^+Cl^-$ and MCPBA as a function of free collidine in CH_3OH. (●) pH 8.25; (+) pH 7.46; 25 °C; [TBPH] = 10^{-2} M; [$\mathbf{1}^+Cl^-$] = 2×10^{-6} M.

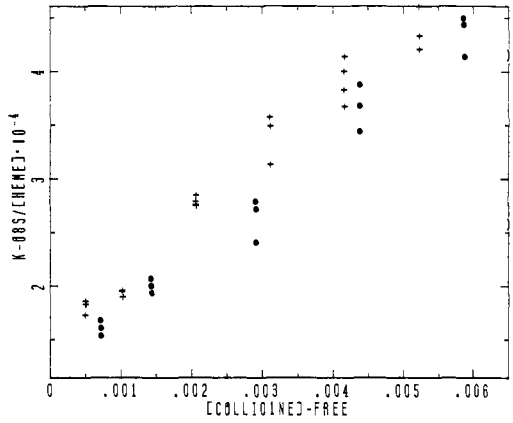

Figure 5. Rate of intermediate formation between $\mathbf{2}^+Cl^-$ and MCPBA as a function of free collidine in CH_3OH. (○) pH 8.25; (+) pH = 7.0; 25 °C; [TBPH] = 10^{-2} M; [$\mathbf{2}^+Cl^-$] = 2×10^{-6} M.

$\mathbf{8}^+Cl^-$ shows a slope k_B, like that for the diester.

Discussion

Groves and co-workers[23] reported that the *m*-chloroperbenzoic acid oxidation of tetramesitylhemin in methanol–methylene chloride produced an oxidized species that transfers an oxygen atom to norbornene.

This suggests a two-electron oxidation of the hemin. Spectroscopic evidence was presented in support of an Fe(IV) porphyrin radical cation for this intermediate. We show (Table I) that this hemin catalyzes tri-*tert*-butylphenol oxidation by *m*-chloroperbenzoic acid with the same bimolecular rate constant as does tetraphenylhemin or protohemin dimethyl ester. Since tetramesitylhemin does not form the μ-oxo species[23] we conclude that, in this and the other examples, we are detecting formation of the monomeric "oxene" species directly.[38a] [The symbol –Fe(=O)⁺– is used for stoichiometry only, i.e., 2 electron equiv oxidized relative to hemin, and not electronic structure.]

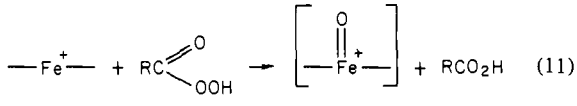

(38) (a) See Traylor, Lee, and Stynes (Traylor, T. G.; Lee, W. A.; Stynes, D. V. *Tetrahedron*, in press) for further evidence. (b) S. Sligar (personal communication) found no CO_2 upon reaction of perphenylacetic acid with HRP, in keeping with previous reports of heterolytic O–O bond cleavage with this enzyme.[3]

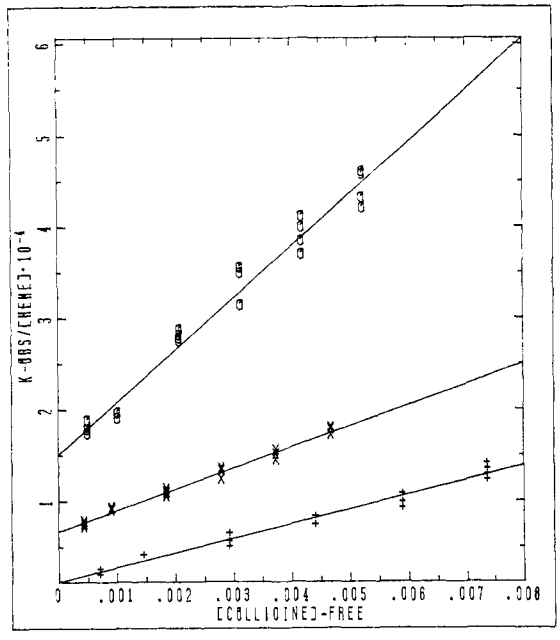

Figure 6. Rate of intermediate formation between model hemin and MCPBA as a function of free collidine at pH 8.25 (collidine/collidine hydrochloride = 5.9). (+) $\mathbf{5}^+Cl^-$; (×) $\mathbf{1}^+Cl^-$; (○) $\mathbf{2}^+Cl^-$; [TBPH] = 10^{-2} M; 25 °C. In the case of [$\mathbf{6}^+Cl^-$] rates are less accurate, about ±30%. Slopes and intercept in Table V.

The stoichiometry of our reactions and our failure to find carbon dioxide with alkyl peracids strongly support this heterolytic cleavage to the acid.[38b] The alternative homolytic process would, in the case of perphenylacetic acid, produce the phenylacetoxy radical, which is known to have essentially no lifetime.

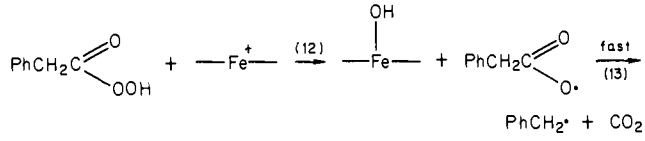

In the case of *tert*-butylperphenylacetate, the thermal homolysis of the oxygen–oxygen bond and the carbon–carbon bond are concerted.[39]

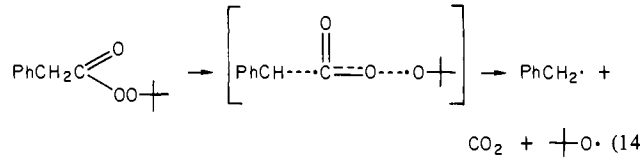

Further support of heterolytic O–O bond cleavage comes from the increased rate with increasing stability of the leaving group (Table IV) as well as the observation of general base catalysis (Figures 4–6). Both observations are consistent with a transition state in which the leaving group is anionic.

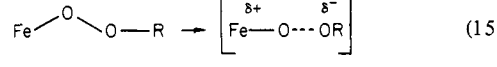

The alternative possibility that the O–O bond breaking and substrate oxidation are concerned (eq 16) requires a dependence upon substrate concentration which we do not find.

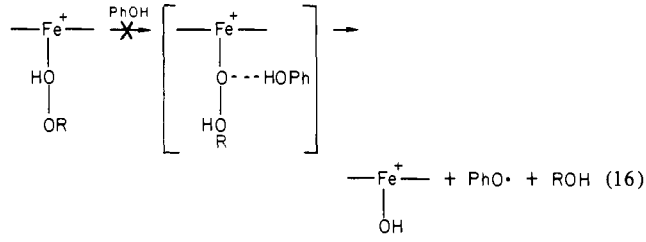

(39) Bartlett, P. D.; Ruchardt, C. *J. Am. Chem. Soc.* **1960**, *82*, 1756–1762.

Table V. Slope and Intercept Values for the Rate of Intermediate Formation as a Function of Collidine and pH for MCPBA and H_2O_2 in CH_3OH at 25 °C

hemin	oxidant	pH	slope, k_B, M^{-2} s^{-1}	intercept, M^{-1} s^{-1}
1^+Cl^-	MCPBA	8.25	$(2.3 \pm 0.1) \times 10^6$	$(6.8 \pm 0.2) \times 10^3$
1^+Cl^-	MCPBA	7.46	$(2.8 \pm 0.1) \times 10^6$	$(6.4 \pm 0.3) \times 10^3$
2^+Cl^-	MCPBA	8.25	$(5.7 \pm 0.2) \times 10^6$	$(1.5 \pm 0.1) \times 10^4$
2^+Cl^-	MCPBA	7.0	$(5.5 \pm 0.2) \times 10^6$	$(1.1 \pm 0.1) \times 10^4$
5^+Cl^-	MCPBA	8.25	$(1.6 \pm 0.2) \times 10^6$	$(1.0 \pm 0.3) \times 10^3$
1^+Cl^-	H_2O_2	8.25	$(2.7 \pm 0.2) \times 10^4$	16.0

The evidence for the initial formation of the "oxene" complex similar to the well-characterized oxene intermediate described by Groves et al.[23] is therefore very strong.

It remains to demonstrate that the production of tri-*tert*-butylphenoxyl radical (RO·) in this catalyzed reaction actually measures the rate of oxene production. The kinetics of reaction in methanol, aqueous methanol, and methylene chloride by using chelated protohemin (1^+Cl^-), as well as those of the other catalysts, are accurately described by the rate law

$$\frac{d[RO\cdot]}{dt} = k_a[1^+Cl^-][\text{peracid}] \qquad (17)$$

The rate is independent of the concentration of the phenol from 10^{-3}–0.1 M, indicating that the phenol reacts with the intermediate as fast as it is formed. The absence of change in the hemin spectrum during the reaction shows that no detectable intermediate accumulates. The sequence of reactions consistent with these findings is

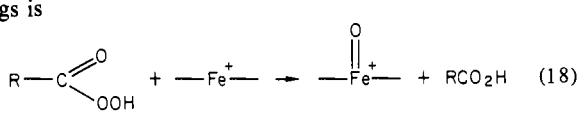

(18)

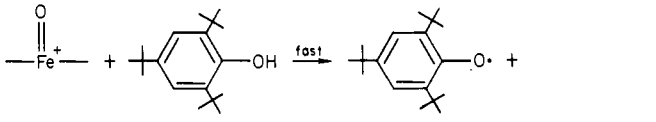

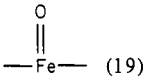

(19)

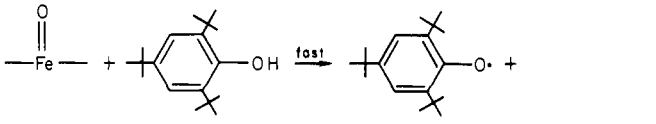

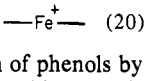

(20)

This finding is consistent with the rapid oxidation of phenols by HRP compounds I and II. While this reaction provides no evidence concerning the reactivity of the intermediate, it does serve as an accurate measure of the rate of intermediate formation without the hemin destruction that occurs in most studies of olefins or hydrocarbon oxidation.[23b,40]

The reaction of hemins in solution is complicated by preequilibria involving the solvent, attached bases, and other ligands that might be present. (B = attached base, solvent, external bases.)

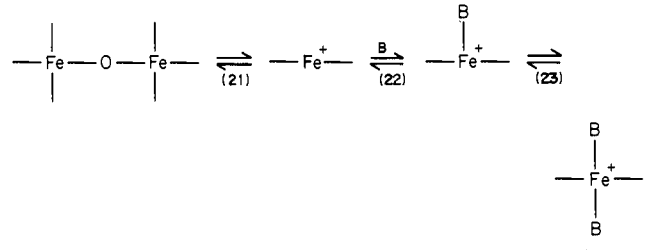

However, variations in these equilibria do not seem to be an important factor in our kinetic studies. It can be seen in Table I that hemins without functional groups, tetramesitylhemin, tetraphenylhemin, protohemin dimethyl ester, and protohemin bis(dimethylamide), all react with MCPBA at the same rate in methanol, the most ligating solvent used. Furthermore, protohemin dimethyl ester (4^+Cl^-) reacts at the same rate in methanol, methylene chloride, and benzene (Table V), indicating no significant solvent effect on hemins not bearing functional groups. It follows that the hemins with appended functional groups owe their increased reactivity to some specific interaction of the appended base, discussed below. Similarly, nonliganding buffers such as collidine/collidine hydrochloride cannot shift the preequilibria with changing buffer concentration. In a given solvent system and using protohemin derivatives we can consider the hemin ligation to remain constant except for internal binding of an attached base. This simplifies the interpretation of the effects of appended functional groups on hemin reactivities.

Rate-Limiting Step. The reaction is first order in peracid over a wide range of concentration with no sign of saturation kinetics. This indicates that either the association step (24) or the oxy-

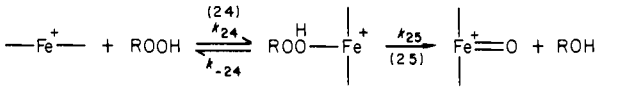

gen–oxygen bond cleavage step (25) is rate limiting. Two observations demand that k_{25} limits the rate. First, associations such as k_{24} are usually fast[41] and are not general base catalyzed as would be required if k_{24} were rate limiting. Second, the rate decreases as R is made electron donating. This would not be the case for the association reaction. Both the association rate and equilibrium constant ($K_{24} = k_{24}/k_{-24}$) would increase with electron donation by R. This finding suggests that K_{24} is much less sensitive to electronic effects than is the cleavage reaction, k_{25}. Because the effects of R on K_{24} and k_{25} are in opposite direction, the effect on k_{25} is larger than our observed effect.

T. Bruice[36] recently reported a correlation of the rates of oxygen transfer from ROOH to sulfides and anilines with the pK_a of ROH, finding that the log k vs. pK_a slope is −0.6. A similar plot of log k vs. pK_a from Table V gives a slope of −0.24. Both reactions can be viewed as a nucleophilic substitution on oxygen by nucleophiles R_2S, R_3N, or Fe^+, displacing RO^- or its hydrogen-bonded form. The reaction with amines and sulfides was viewed as an S_N2 process, whereas the hemin-catalyzed process is proposed to be an AS_N2 process. We are presently attempting to demonstrate the reversible addition of ROOH or ROO^- to hemins (eq 24).

General Base Catalysis. The finding that collidine or carboxylates[27] accelerate the rate of the peroxide cleavage is consistent with a transition-state stoichiometry comprising hemin, peracid, and base. A reasonable geometry for such a structure would have the conjugate acid of the base bonding to the leaving group.

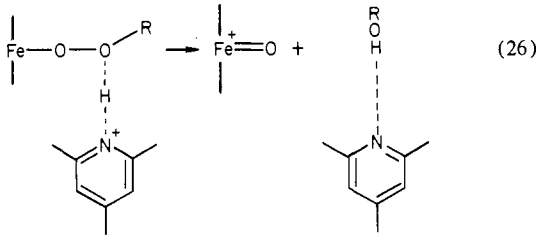

(26)

General base catalysis by carboxylates should result in autocatalysis of the reaction as a result of the production of acid from the peracid cleavage. In our systems the acid does not reach sufficient concentration for such catalysis to be detectable and we observe no autocatalysis at the highest peracid concentrations (5×10^{-4} M).

The enzymatic utilization of such hydrogen bonding invariably involves an attached base that is held in juxtaposition for maximal

(40) Chang, C. K.; Kuo, M. S. *J. Am. Chem. Soc.* **1979**, *101*, 3413–3415.

(41) The reaction of peracids with the sterically hindered hemin in HRP requires association rates in excess of 10^8 M^{-1} s^{-1}.

H bonding. We therefore tested for such internal effects by attaching bases to the hemin. In some cases the base could also bind directly and internally to the iron and thus provide a proximal base effect. It is therefore of some interest to separate these two possibilities.

Distal Base Catalysis (Internal GBC). Table I reveals rate constants of 2×10^3 M^{-1} s^{-1} for protohemin dimethyl ester, 5×10^4 M^{-1} s^{-1} for the monomethyl ester, and 9×10^4 M^{-1} s^{-1} for protohemin itself. Jones[29] reported that coprohemin (a tetracarboxylic acid) reacts with hydrogen peroxide faster than does mesohemin (a dicarboxylic acid). Since these reactions are carried out in an excess of developing carboxylic acid (from the peracid), no external effect of low concentration hemin carboxylic acid is expected. However, as Jones[27] has suggested, carboxylic acid anions can act as general bases in the manner described for collidine. We have shown that appended bases in chelated hemes display an effective local concentration of 0.1–0.2 M in the vicinity of the heme.[42] Thus, the propionate side chain provides an internal base for catalysis.[43]

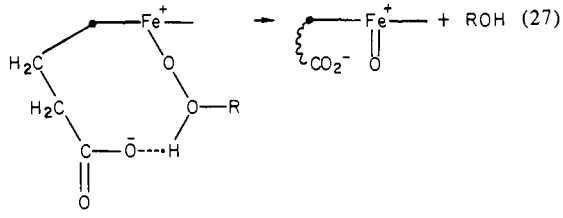

However, it cannot bind to iron. Notice that a second propionic acid ($\mathbf{8}^+Cl^- \rightarrow \mathbf{9}^+Cl^-$) increases the rate whereas a second liganding imidazole ($\mathbf{5}^+Cl^- \rightarrow \mathbf{6}^+Cl^-$) reduces the rate.

Assigning the rate constant for protohemin dimethyl ester as k_o, we can write the rate constant, k_m, for the monoester ($\mathbf{8}^+Cl^-$) as

$$k_m = k_o + k_{B_i}B_i \tag{28}$$

where k_{B_i} is the rate constant for the internal base and B_i its effective concentration. Adding an external base such as collidine (B) would simply add another term (eq 29) since the two catalyses

$$k_m' = k_o + k_{B_i}B_i + k_BB \tag{29}$$

are competitive. This is similar to the addition of external base to the diester (eq 30) and the k_BB term would be identical. Taking

$$k_o' = k_o + k_BB \tag{30}$$

the value of $k_B = 1.6 \times 10^6$ M^{-2} s^{-1}, the increase in rate for k_m at 0.005 M would be 8×10^3 M^{-1} s^{-1} added to the rate constant 5×10^4 M^{-1} s^{-1}. We observed the same rate for the monoester at 0 and 0.005 M collidine, consistent with this analysis (see Table I). If the slope were proportional to the accelerated rate k_m, i.e., about six times that for $\mathbf{1}^+Cl^-$, rather than k_o, the expected rate increase would be about 6×10^4 M^{-1} s^{-1}, which was not observed. Although the rates observed for the monoacid $\mathbf{8}^+Cl^-$ were subject to greater errors (±20%) than were other rates, the results are clearly consistent with eq 29.[45] Further evidence for a qualitative difference between side chains that can or cannot bind internally to iron is presented below.

Proximal Base Effects. By contrast to the analysis for distal base effect (internal general base catalysis), the proximal base effect, being an electronic acceleration of O–O bond breaking, would be cooperative with rather than competitive with external GBC. Thus, if chelated hemins were accelerated by a multiplicative factor, γ, over protohemin dimethyl ester, then the rate for these hemins, k_{ch}, in the absence of external bases would be written

$$k_{ch} = \gamma k_o \tag{31}$$

and that in the presence of the external general base would be

$$k_{ch}' = \gamma k_o + \gamma k_B{}^*B \tag{32}$$

In this case the observed slopes of the k_{ch}' vs. collidine plots would increase as the uncatalyzed rate (k_{ch}) increases, although $k_B{}^*$ might not be exactly the same as k_B.

Table V shows the slopes of both $\mathbf{1}^+Cl^-$ (2.3×10^6 M^{-2} s^{-1}) and $\mathbf{2}^+Cl^-$ (5.7×10^6 M^{-2} s^{-1}), the chelated hemins, to be significantly greater than that of the diester $\mathbf{5}^+Cl^-$ (1.6×10^6 M^{-2} s^{-1}). We conclude that both $\mathbf{1}^+Cl^-$ and $\mathbf{2}^+Cl^-$ accelerate the peroxide cleavage through electron donation by a proximal base. This

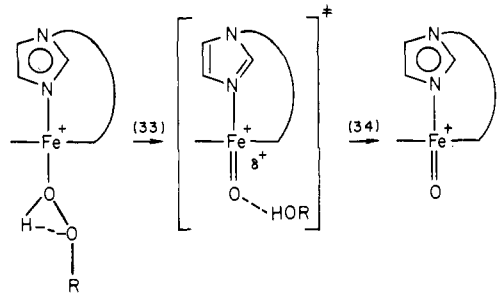

conclusion is corroborated by the large k_{ch}/k_o ratios observed in benzene and methylene chloride.

When a distal base, a proximal base, and an external base are present, the rate constant should be

$$k_{ch}'' = \gamma k_o + \gamma k_{B_i}{}^*B_i + \gamma k_B{}^*B \tag{35}$$

If the γk_o and $\gamma k_B{}^*B$ terms are the same as with $\mathbf{1}^+Cl^-$, then $\gamma k_B{}^*B$ would be 1.2×10^4 M^{-1} s^{-1} at 0.005 M collidine. The rate constant for $\mathbf{7}^+Cl^-$ without collidine is 1×10^5 M^{-1} s^{-1}. Addition of 0.05 M collidine left this rate essentially unchanged within the error (±15%) in these measurements, consistent with a combination of proximal (imidazole) and distal (COO^-) effects. The replacement of a carboxylate group in $\mathbf{7}^+Cl^-$ with a chelating imidazole group to produce the diimidazole compound $\mathbf{6}^+Cl^-$ results in a decrease of 30 in the rate constant, indicating proximal base binding of the imidazole arms.

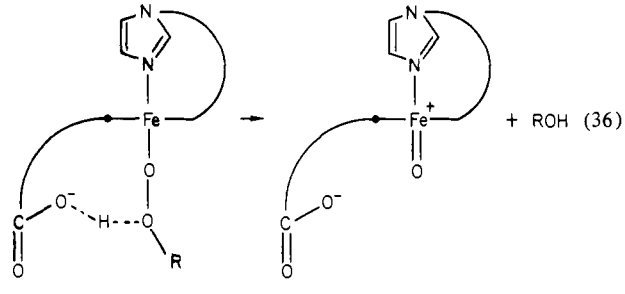

It is clear that compounds having appended bases with sufficient chain length to allow internal binding (capable of proximal base effects) are characterized by increased general base catalysis constants, k_B, as compared to either the simple hemin ($\mathbf{4}^+Cl^-$) or those bearing side chains too short for internal binding but capable of internal general base catalysis.

The proximal and distal effects are summarized in Scheme I where the numbers over the arrows refer to acceleration factors upon making the indicated change.

The proximal effects in methanol are rather small. However, these effects are much larger in less polar and less liganding solvents such as methylene chloride or benzene (Table III). In these nonpolar solvents the internal base tends to bind much more strongly than it does in polar solvents.[42]

(42) Geibel, J. Thesis, University of California, San Diego, 1976.
(43) Preliminary studies indicate that protohemin monomethyl ester mono(4-imidazolyl)methylamide, which, like the propionate, cannot internally bind to iron,[44] accelerates the rate of peracid reduction.
(44) Traylor, T. G.; Mitchell, M. J.; Ciccone, J. P.; Nelson, S. *J. Am. Chem. Soc.* **1982**, *104*, 4986–4989.
(45) T. Asakura and T. Yonetani (*J. Biol. Chem.* **1969**, *244*, 4573–4579) have shown that esterification of the propionic acids on the hemin in CCP does not decrease the rate of reaction with hydrogen peroxide, indicating that the enzyme uses the distal imidazole but not the propionate as a general base catalyst.

Scheme I. Acceleration Factors due to Side Chain Alterations: The Data Are from Table I

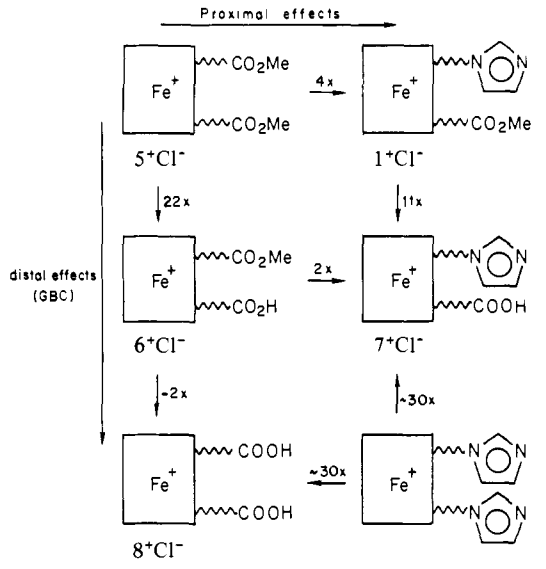

The mechanism of formation of the oxene intermediate, –Fe-(=O)$^+$–, can now be written as

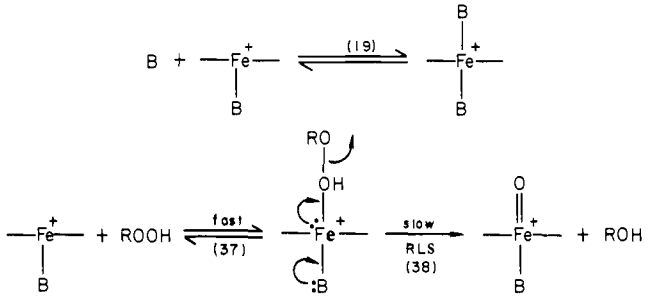

The rate is accelerated by electron donation by the proximal base, B, by increased stability of the leaving anion RO^-, and by general base catalysis that functions to increase the leaving ability of RO^-. It is retarded by binding of a second base, B, to the hemin just as in the case of HRP.[1]

Relevance of the Model Reaction to Peroxidase Reaction. Having employed protohemin derivatives as model systems we can assume the same electronic factors as those operating in horseradish peroxidase (HRP) and cytochrome *c* peroxidase (CCP). The chelated hemins also have the same proximal base as do the enzymes. However, internal binding of the base is enforced in the enzyme and only partially enforced in the models. In the latter case the local concentration is equivalent to about 0.2 M[42] compared to a very high (>20 M) equivalent local concentration in the proteins.[46]

The enormous difference in the rate of hydrogen peroxide reaction with **1**$^+$Cl$^-$ in methanol (12 M^{-1} s^{-1}) compared to that with HRP (1.8×10^7 M^{-1} s^{-1})[18,20] or CCP (1.4×10^8 M^{-1} s^{-1})[34] suggests an extraordinary catalysis, additional to the presence of the pentacoordinated hemin. Furthermore, the large difference between the reactivity of H_2O_2 and MCPBA observed with chelated protohemin in methanol (12 M^{-1} s^{-1} vs. 7600 M^{-1} s^{-1}, respectively) almost disappears in their reactions with HRP (1.8×10^7 M^{-1} s^{-1} and 1.2×10^8 M^{-1} s^{-1}).[18,20]

Three kinds of effects have been suggested[1,3,47a] for the catalysis based upon the chemical studies of HRP[1] and CCP[3] and on the crystal structure of CCP recently determined by Poulos et al.[47] The active site has a glutamate residue near the proximal imidazole, a distal imidazole in position for hydrogen bonding, and an arginine on the distal side. On the basis of these peculiarities, which differ from the environment in myoglobin except for the distal imidazole, the following transition-state geometry was suggested.[47]

Chart I

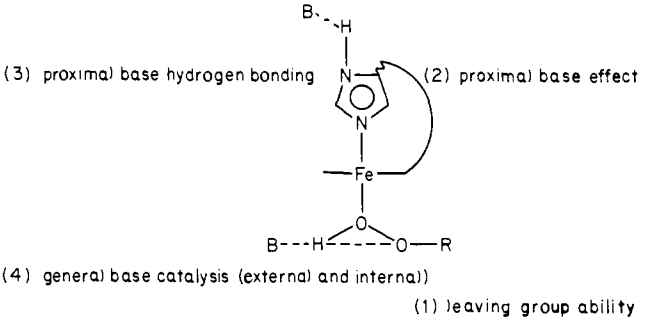

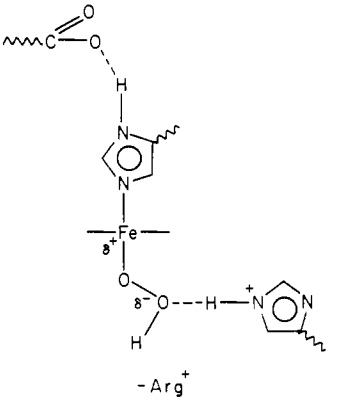

We have not demonstrated the arginine effect yet but our observation of general base catalysis confirms the H-bonding effect proposed for CCP. The larger sensitivity (k_B/intercept) for general base catalysis of the hydrogen peroxide reaction (1700 M^{-1}) than that for the MCPBA reaction (340 M^{-1}) (see Table V) helps to explain the disappearance of the dependence on peroxide structure with HRP or CCP.

We also tentatively suggest that the larger rate constant observed with **2**$^+$Cl$^-$, which has a proximal imidazole proton, than with **1**$^+$Cl$^-$, which does not, is consistent with hydrogen bonding of this proton, which increases the electron density at iron and consequently the rate of O–O bond cleavage. This offers a function for the glutamate found near the proximal imidazole in CCP.[47]

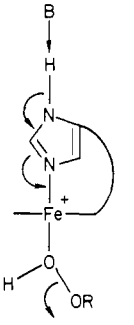

It is interesting to compare absolute rates of reaction of the models and those of HRP. The rate of the general base catalyzed reaction of **1**$^+$Cl$^-$ with MCPBA (7.6×10^3 M^{-1} s^{-1}) can be extrapolated to that of HRP (1.2×10^8 M^{-1} s^{-1})[20] at 21 molar collidine. This is a reasonable effective concentration of a neighboring base in the enzyme. The same extrapolation for the reaction of **1**$^+$Cl$^-$ with hydrogen peroxide in methanol (12 M^{-1} s^{-1}) would require 670 molar collidine to equal the rate constant in HRP (1.8×10^7 M^{-1} s^{-1}). However, a change from **1**$^+$Cl$^-$ to **2**$^+$Cl$^-$ and from methanol to methylene chloride should increase

(46) Fersht, A. R.; Kirby, A. J. *J. Am. Chem. Soc.* **1967**, *89*, 4857–4863.
(47) (a) Poulos, T. L.; Kraut, J. *J. Biol. Chem.* **1980**, *255*, 8199–8205. (b) Poulos, T. L.; Freer, S. T.; Alden, R. A.; Edwards, S. L.; Skogland, U.; Takio, K.; Eriksson, B.; Xuong, N.; Yonetani, T.; Kraut, J. *J. Biol. Chem.* **1980**, *255*, 575–580.

the rate by at least a factor of 30. Therefore, a combination of the proximal, distal, and solvent effects reported here would suffice to bring about a reaction of hydrogen peroxide that is equivalent to those of the enzymes.

Conclusion

We have devised a model for peroxidase reactions with hydrogen peroxide or peracids in which protohemin derivatives catalyze a high turnover oxidation of 2,4,6-tri-*tert*-butylphenol. Several of the catalytic effects proposed for peroxidases have been demonstrated with this model system. These are listed in Chart I. Mechanisms of reaction of the intermediate with phenols is discussed elsewhere.

Experimental Section

Materials. Model compounds $\mathbf{1}^+Cl^-$, mesohemin–$\mathbf{1}^+Cl^-$, $\mathbf{4}^+Cl^-$, and $\mathbf{8}^+Cl^-$ were prepared according to published procedures.[32] Model compounds $\mathbf{3}^+Cl^-$,[48] $\mathbf{5}^+Cl^-$,[49] $\mathbf{6}^+Cl^-$,[32] and $\mathbf{7}^+Cl^-$[50] were those used in previous studies. Tetraphenylporphyrin (Aldrich) was used as received. Tetramesitylporphyrin was also prepared according to published procedures.[51] Iron insertions were carried out by published methods.[52]

Purities of all oxidizing agents, given in parentheses, were determined by iodometric analysis.[53] At the same calculated concentration of *m*-chloroperbenzoic acid (MCPBA), identical rates were obtained by using either commercial MCPBA (81%) (Aldrich) or that which had been washed by extraction with pH 7.2, phosphate buffer and recrystallized from hexane–diethyl ether, 3:1, to yield 98% active material. Perlauric acid (98%)[54] and phenyl peracetic acid (91%)[55] were prepared as described in the literature. *p*-Nitroperbenzoic acid (84%) and *tert*-butylhydroperoxide (75%) were obtained from the Aldrich Chemical Co. and used as received. The H_2O_2 (30%) was from Mallinckrodt. Potassium *m*-chloroperbenzoate was prepared by stirring potassium in dry benzene and adding 1 equiv of MCPBA. The white solid formed was isolated by decanting the benzene solution.

2,4,6-Collidine, purified grade, was purchased from Sigma and reported to be 99.9% pure by gas chromatography. Collidine hydrochloride was prepared by bubbling technical-grade HCl gas through collidine (9.1 g, 74.6 mmol) in 40 mL of anhydrous diethyl ether. The white solid was filtered, dried (9.5 g), and recrystallized from absolute EtOH (2 mL/g).

Anhydrous methanol was Mallinckrodt Spectra AR grade and was not purified further. Methylene chloride was distilled under argon from CaH_2 and stored over 4-Å molecular sieves. Benzene solutions were prepared by using Mallinckrodt Spectra AR grade benzene. Tri-*tert*-butylphenol (Aldrich) was recrystallized twice from 95% EtOH. Methanol–water solutions (80:20, 60:40) were prepared by using triply glass distilled water and mixed volume/volume. Dimethylformamide was distilled from CaH_2 and stored over 4-Å molecular sieves. All other reagents were used as received from the manufacturer.

Kinetic Data. All stopped-flow measurements were done on an Aminco-Morrow stopped-flow instrument.[56] Rates were determined by following the transmittance change at or near the Soret maximum for the specific hemin complex and at 400 and 630 nm for the tri-*tert*-butylphenoxyl radical. The voltage output from the photomultiplier was recorded digitally through a microprocessor and rate constants were obtained as described elsewhere.[57] The temperature of the mixing block was kept at 25 ± 0.2 °C with a circulating water bath.

For determination of the rate law for oxidation of TBPH in CH_3OH–H_2O (80:20) and CH_3OH–H_2O (60:40), the production of phenoxyl radical was monitored at 630 and 400 nm. The radical is stable enough in CH_3OH–H_2O (80:20) to make deoxygenating the solutions unnecessary. Two methods of mixing the reagents on the stopped-flow apparatus were employed: (*1*) the MCPBA and TBPH were premixed in one drive syringe and the $\mathbf{1}^+Cl^-$ in the other; (*2*) $\mathbf{1}^+Cl^-$ and TBPH were premixed and flowed against the MCPBA. Both methods gave identical results. The direct reaction between $\mathbf{1}^+Cl^-$ and MCPBA in CH_3OH–H_2O (80:20) was also measured on the stopped-flow instrument. The observed Δtransmittance vs. time curves clearly showed a biphasic process. The pseudo-first-order rate constants were calculated by selecting a best-fit A_∞ value for the first process. This led to large deviations in the direct analysis.

Rate experiments where the second-order rate constants were less than 1×10^5 M^{-1} s^{-1} were measured either on the Cary 15 spectrophotometer at a selected wavelength and fixed chart speed or on a Kontron Uvikon 810/820 instrument. The plot of absorbance vs. time obtained from the Cary 15 was converted to pseudo-first-order rate constants by manual digitization of the spectra and plotting ln $(\Delta A_\infty - \Delta A_0)$ vs. time where the slope is the pseudo-first-order rate constant. The temperature in the brass cell holder was kept at 25.0 ± 0.1 °C by a circulating water bath. The Uvikon 810/820 is capable of a digital output that can be processed through existing programs to obtain the pseudo-first-order rate constants. The temperature in the cell compartment of the Uvikon was maintained at 25.0 ± 0.1 °C by using a water-jacketed cell holder.

All kinetic runs in which the phenoxyl radical concentration was measured in pure methanol, benzene, dimethylformamide, and methylene chloride were done on the Cary 15 or the Uvikon 810/820. This includes runs where the oxidant type and the hemin model were varied.

Typically, 5 mL of a 1.0×10^{-3} M solution of tri-*tert*-butylphenol in CH_3OH was added to an 8-in. 1-cm path length silica cuvette. A septum was placed over the cuvette and an appropriate amount of a concentrated hemin solution was injected (5–10 μL) to give the desired concentration as determined by the absorbance of the Soret. The solution was then deoxygenated by blowing through it solvent-saturated argon for 10 min. To this solution, 1–10 μL of a 0.10 M solution of peracid was injected, and the solution was shaken vigorously and placed in the spectrophotometer, where absorbance vs. time was measured. The fastest half-life under pseudo-first-order conditions that could be measured accurately was 8 s.

Spectral Intermediate. The spectral intermediate formed in the reaction of $\mathbf{1}^+Cl^-$ and MCPBA in CH_3OH–H_2O (80:20) was determined on the stopped-flow apparatus. Solutions of $\mathbf{1}^+Cl^-$ (9.1×10^{-5} M) and potassium *m*-chloroperbenzoate (2.5×10^{-4} M) were flowed together at 25 °C. The intermediate spectra were determined by monitoring the change in transmittance with time at 330, 350, 370, 380, 390, 394, 398, 404, 410, 420, 430, and 440 nm. These data were then compiled to give absorbance vs. wavelength at specific time intervals. There was a rapid decrease in the Soret absorption with isosbestic points at 345 and 420 nm followed by a slower disappearance of the entire spectrum.

Oxidation Equivalents of Intermediate. A 10-mL solution of 1.0 M TBPH in CH_2Cl_2 was prepared and transferred to a 130-mL tonometer. Mesohemin–$\mathbf{1}^+Cl^-$ was added to the solution to give a 1×10^{-5} M solution in hemin. A small stir bar was added to the tonometer, and the solution was sealed and degassed by three freeze–pump–thaw cycles and finally placed under argon. A separate 0.0125 M MCPBA solution in CH_2Cl_2 was also prepared and degassed by three freeze–pump–thaw cycles. While the mixture was stirred rapidly, four 0.5-mL injections of the MCPBA solution were added to the tonometer. The production of tri-*tert*-butylphenoxyl radical was monitored at 630 nm (ε 400). A similar experiment was repeated in CH_3OH.

Homolytic vs. Heterolytic Cleavage of Peracid. Two 100-mL three-necked round-bottom flasks equipped with stirring bars were connected with Tygon tubing. Attached to flask 1 was a nitrogen line and to flask 2 an oil bubbler. Flask 1 contained a solution of 0.5 M TBPH and 5×10^{-4} M mesohemin–$\mathbf{1}^+Cl^-$ in 50 mL of CH_2Cl_2 and flask 2 contained a 100-mL solution of standardized $Ba(OH)_2$. Nitrogen was passed over the stirred solution in flask 1 and led through the solution in flask 2. A dropping funnel containing 25 mL of CH_2Cl_2 and 0.0889 g (4×10^{-4} mol) of perlauric acid was attached to flask 1. The perlauric acid was added dropwise over a period of 90 min to the rapidly stirring hemin–TBPH solution while maintaining a nitrogen gas flow rate of 1 mL/min. A control experiment was also set up by bubbling nitrogen through a separate hemin–TBPH solution and into a $Ba(OH)_2$ solution at the same rate. After 90 min a 5-mL aliquot was removed from flask 1 and the visible spectra were recorded. The ratio of phenoxyl radical to perlauric acid was 1.5:1. Three 25-mL aliquots were then removed from the $Ba(OH)_2$ solution and from the control solution. Both were titrated with standardized HCl solution and no significant difference (1.5%) was found in the $BaCO_3$ content. Ten milliliters of CO_2 gas was then injected into the control flask over a period of 30 min. Almost immediately a white flocculant precipitate appeared in the $Ba(OH)_2$ solution. Titration of the

(48) Geibel, J.; Cannon, J.; Campbell, D.; Traylor, T. G. *J. Am. Chem. Soc.* **1978**, *100*, 3575–3584.
(49) Berzinis, A. P., Ph.D. Thesis, University of California, San Diego, 1979.
(50) Traylor, T. G.; Mincey, T. C.; Berzinis, A. P. *J. Am. Chem. Soc.* **1981**, *103*, 7084–7089.
(51) Alder, A. D.; Sklar, L.; Longo, F. R.; Finarelli, J. D.; Finarelli, M. G. *J. Heterocycl. Chem.* **1968**, *5*, 669–678.
(52) Adler, A. D.; Longo, F. R.; Kampas, F.; Kim, J. *J. Inorg. Nucl. Chem.* **1970**, *32*, 2443–2445.
(53) Mair, R. D.; Graupner, A. J. *Anal. Chem.* **1964**, *36*, 194–204.
(54) Parker, W. E.; Ricciutti, C.; Ogg, C. L.; Swern, D. *J. Am. Chem. Soc.* **1955**, *77*, 4037–4041.
(55) McDonald, R. N.; Steppel, R. N.; Dorsey, J. E. *Org. Synth.* **1970**, *50*, 15–18.
(56) White, D. K.; Cannon, J. B.; Traylor, T. G. *J. Am. Chem. Soc.* **1979**, *101*, 2443–2454.
(57) Traylor, T. G.; Campbell, D.; Sharma, V.; Geibel, J. *J. Am. Chem. Soc.* **1979**, *101*, 5376–5383.

$Ba(OH)_2$ showed that 77% of the CO_2 was trapped. Phenylperacetic acid was also examined by using the identical procedure.

Rate of Intermediate Formation by *tert*-Butyl Hydroperoxide and H_2O_2. Two methods were employed to determine the rate of intermediate formation by *tert*-butyl hydroperoxide and H_2O_2. (1) In CH_3OH, 5-mL samples of 1.5×10^{-5} M $\mathbf{1}^+Cl^-$ were prepared in 1-cm silica cuvettes. To these solutions was added via a microliter syringe 100, 50, or 10 μL of a 1.0 M *tert*-butyl hydroperoxide solution or H_2O_2. The rapid decrease in absorbance vs. time was followed. By use of the initial rate method, the rate constant for intermediate formation was calculated. (2) In CH_3OH, 5-mL solutions of 1.5×10^{-5} M $\mathbf{1}^+Cl^-$ and 0.5 M TBPH were prepared and deoxygenated with solvent-saturated argon. To these solutions, 100 and 50 μL of 1.0 M *tert*-butyl hydroperoxide or H_2O_2 was injected and the increase in absorbance vs. time monitored. The initial rate method was then used to determine the rate constant for intermediate formation.

Preparation of Mesohemin-2-(4-Imidazoyl)ethylamide Monodioctylamide ($\mathbf{2}^+Cl^-$). Mesohemin (0.45 g, 0.69 mmol) was weighed into a 250-mL three-necked round-bottom flask equipped with stir bar and gas inlet valves. Pyridine, 125 mL, freshly distilled under N_2, was added to the flask and the flask cooled and stirred in an ice–water bath. The addition of pivalyl chloride (500 μL, 2.1 mmol) resulted in the complete conversion to dianhydride as monitored by quenching an aliquot in CH_3OH and examining TLC behavior.

Di-*n*-octylamine (0.22 g, 0.91 mmol) was then added to the reaction mixture at 0 °C. After the mixture was quenched, an aliquot in CH_3OH, TLC on silica gel in $CHCl_3$–CH_3OH (9:1) showed a statistical distribution of mono- and disubstituted hemin.

Histamine (0.40 g, 2.7 mmol) was dissolved in 30 μL of dry benzene and the solution refluxed with a Dean-Stark trap to remove the H_2O. The benzene solution was then poured into the reaction mixture and the solution warmed to room temperature. After being stirred for 1 h at room temperature the reaction mixture was placed on a rotoevaporator and the solvent removed. A solution of 800 mL of 0.1 M HCl and 0.1 M NaCl was added to the residue and the mixture extracted 3× with $CHCl_3$. Removal of $CHCl_3$ yielded a reddish amorphous solid. The compound was purified by column chromatography on silica gel, using 95:5 $CHCl_3$–CH_3OH to elute the bis(dioctylamine) product and 85:15 $CHCl_3$–CH_3OH to elute the monohistamine, monodioctylamine product. The product was characterized by its UV–visible spectra as the imidazole–Fe^{II} species and the imidazole–Fe^{II}–CO species:[31,32] yield 0.12 g (20%): NMR (Fe^{II}–CO complex, CD_2Cl_2): δ 1.3 [m, $-(CH_2)_6-CH_3$], 0.8 [m, $-(CH_2)_6-CH_3$], 3.45 [m, P–CH_3], 10.1 [m, meso, P–H].

Preparation of 2,6-Di-*tert*-butyl-4-[(2-cyano)isopropyl]phenol. 2,6-Di-*tert*-butyl-4-isopropenylquinone methide[58] (2.0 g, 8.1×10^{-2} mol) was dissolved in 50 mL of diethyl ether in a 250-mL round-bottom flask. Potassium cyanide (6 g, 0.09 mol) was dissolved in 10 mL of H_2O and diluted to 50 mL with 95% ethanol. The two solutions were combined and stirred for 12 h at 65 °C in a water bath. The reaction was worked up by diluting with 100 mL of H_2O and extracting the organic layer with 100 mL (3×) of diethyl ether. Removal of the solvent yielded an off-white solid. Recrystallization from 95% ethanol gave white crystals (1.22 g, 55%): mp 126–128 °C; NMR δ 1.4 (s, 14), 1.7 (s, 6), 5.1 (s, 1), 7.2 (s, 2).

Preparation of [2-Methyl-2-[3,5-di-*tert*-butyl-4-hydroxyphenyl]propyl]ammonium Chloride. 2,6-Di-*tert*-butyl-4-[(2-cyano)isopropyl]-phenyl (1.2 g, 4.4×10^{-3} mol) was dissolved in 25 mL of anhydrous diethyl ether in a flame-dried dropping funnel. Lithium aluminum hydride (0.2 g, 5.3×10^{-3} mol) was added to 100 mL of anhydrous diethyl ether in a flame-dried three-necked 250-mL round-bottom flask equipped with stir bar and water bath. The phenol was added to the LAH solution at 0 °C and stirred for 12 h. The reaction was quenched by adding the reaction mixture to 300 mL of 10% NaOH. The mixture was then extracted with 100 mL (3×) diethyl ether, washed with 100 mL of H_2O (3×), and dried over $MgSO_4$. Evaporation of the solvent yielded white crystals (0.6 g, 50%): NMR with added CF_3COOH δ 1.45 (s, 26), 3.2 (q, 2), 6.2 (b, 2), 7.1 (s, 2). The amine was dissolved in diethyl ether and precipitated out as the ammonium chloride salt by bubbling in dry HCl gas (mp dec >240 °C). Elemental anal.: C, 68.75 (68.87); H, 10.55 (10.27); N, 4.8 (4.46); Cl, 11.6 (11.29).

(58) Cook, C. D.; Norcross, B. E. *J. Am. Chem. Soc.* **1956**, *78*, 3797–3799.

General Base Catalysis by Collidine. All of the reactions carried out at fixed pH were done in collidine buffers. The pH was calculated from the ratio of the free base to the conjugate acid.[37] Typically, a pH 7.5 buffer was prepared by dissolving collidine (0.1180 g, 5.01 mmol) and collidine hydrochloride (0.1614 g, 4.99 mmol) in 200 mL of anhydrous spectral-grade CH_3OH containing 10^{-2} TBPH (0.525 g, 2.0 mmol).

Each individual sample was prepared for kinetic analysis by pipetting fixed volumes of the stock buffer solution into 8-in., 1.0-cm path length silica cuvettes and diluting to 5 mL with a stock 10^{-2} M TBPH solution in CH_3OH. In this way, the concentration of buffer was varied by a factor of 10. Each cuvette was then capped with a rubber septum and CH_3OH-saturated argon blown through the sample. A concentrated solution of hemin model was added with a microliter syringe after the solution was saturated with argon and after the absorbance at the particular wavelength of the Soret had been recorded. To ensure the hemin had not been destroyed or modified, a concentrated sample was prepared before every series of runs and its visible spectrum carefully examined. The addition of MCPBA and the recording of the ΔOD vs. time was identical with the procedure described above.

To examine the effect of ionic strength on the rate decomposition of MCPBA, NaCl (0.117 g, 2 mmol) was added to a solution of 200 mL of 5×10^{-3} M collidine buffer at pH 7.5 and 10^{-2} M TBPH. The oxidation of phenol was carried out in the above described manner at 5×10^{-4} M buffer and 5×10^{-3} M buffer, both containing 10^{-2} M NaCl. The rates were identical with those obtained with no NaCl present.

The rate of TBPH oxidation by H_2O_2 catalyzed by $\mathbf{1}^+Cl^-$ was followed by the initial rate method. Samples (10 μL) of a 0.097 and a 0.97 M solution of H_2O_2 were syringed into 5-mL solutions of 7.5×10^{-4} and 7.5×10^{-3} M free collidine at pH 8.25. The ΔOD vs. time was followed for the first 10% of the calculated ΔOD change or until some curvature in the line was noted. Since phenoxyl radical buildup was being monitored, the rate constant obtained by initial rate methods is $2k_1$.

$$v = \frac{d[\text{phenoxyl}]}{dt} = 2k_1[H_2O_2][\text{hemin}] \quad (39)$$

At 7.5×10^{-3} M collidine and 2.0×10^{-4} M H_2O_2 the rate could also be analyzed by pseudo-first-order kinetics as described for the MCPBA oxidations. The decomposition of H_2O_2 by model $\mathbf{7}^+Cl^-$ was examined at 7.5×10^{-4} M free collidine, pH 8.25, also by using a pseudo-first-order kinetic analysis. Samples were prepared in the same manner as described above.

Titration of $\mathbf{1}^+Cl^-$ and $\mathbf{5}^+Cl^-$ with 1-Methylimidazole. Model compounds $\mathbf{1}^+Cl^-$ and $\mathbf{5}^+Cl^-$ were titrated with 1-methylimidazole in CH_3OH at 25 °C. To break up the μ-oxo species formed in CH_3OH, the solution was made 10^{-4} M in *m*-chlorobenzoic acid. This results in the formation of the monoimidazole hemin complex or the methanol-bound hemin (398, 397, 626 nm). Microliter quantities of stock 0.1 and 1.0 M 1-methylimidazole were added and the spectrum was recorded. The data were also stored digitally every 0.5 nm and this output was used to calculate the ΔOD values. The second base-binding constant, K_2, for $\mathbf{1}^+Cl^-$ and 1-methylimidazole was calculated at four wavelengths (396, 396, 540, 630 nm) by using the relationship $K_2 = (A_t - A_\infty)/(A_\infty - A_t)[B]$. Only values of $(A_t - A_\infty)/(A_\infty - A_t)$ between 0.3 and 3.0 were used in the calculations.

Acknowledgment. We are grateful to the National Science Foundation (Grant CHE 81-20969) for financial support. Some of the computer applications derived support from the National Institutes of Health (Grant RR-00757).

Registry No. $\mathbf{1}^+\cdot Cl^-$, 87985-22-6; mesohemin-$\mathbf{1}^+\cdot Cl^-$, 87985-23-7; $\mathbf{2}^+\cdot Cl^-$, 87985-24-8; $\mathbf{3}^+\cdot Cl^-$, 87985-25-9; $\mathbf{4}^+\cdot Cl^-$, 15741-03-4; $\mathbf{5}^+\cdot Cl^-$, 87985-26-0; $\mathbf{6}^+\cdot Cl^-$, 87999-34-6; $\mathbf{7}^+\cdot Cl^-$, 87985-27-1; $\mathbf{8}^+\cdot Cl^-$, 42279-41-4; $\mathbf{9}^+\cdot Cl^-$, 16009-13-5; iron(III) tetraphenylporphyrin chloride, 14187-12-3; iron(III) tetramesitylporphyrin chloride, 77439-21-5; TBPH, 732-26-3; MCPBA, 937-14-4; H_2O_2, 7722-84-1; *p*-nitroperbenzoic acid, 943-39-5; perlauric acid, 2388-12-7; *tert*-butyl hydroperoxide, 75-91-2; mesohemin, 21007-37-4; di-*n*-octylamine, 1120-48-5; histamine, 51-45-6; 2,6-di-*tert*-butyl-4-[2-cyanoisopropyl]phenol, 87970-43-2; 2,6-di-*tert*-butyl-4-isopropenylquinone methide, 87970-44-3; [2-methyl-2-[3,5-di-*tert*-butyl-4-hydroxyphenyl]propyl]amine hydrochloride, 87970-45-4; 1-methylimidazole, 616-47-7; peroxidase, 9003-99-0.